Presented at Loughborough Antennas & Propagation Conference, Loughborough, 16th - 17th November 2009

Microstrip Antennas Utilizing MEMS for Reconfigurable Polarisation States

Ivor L. Morrow[#1], D. H. Schaubert[#2], N. Clow[#3]

[#1]*Cranfield University, Shrivenham, UK*

[#2]*University of Massachusetts, Amherst, USA*

[#3]*Dstl, Fort Halstead, UK*

***Abstract*— A modern approach to an established technique is investigated for the electronic control of polarisation of microstrip patch antennas. The control is achieved by placing micro-electromechanical switches (MEMS) at appropriate locations in a patch antenna. The microwave MEMS are used to switch between open and short circuit conditions that allow reconfiguration of the modal fields. Changing the number and location of short circuit field regions changes the radiated field polarisation from linear horizontal to vertical, right hand circular or left hand polarisation. All of the polarisation states are obtained without changing the frequency of operation, input impedance or radiation pattern of the patch antenna. The antenna is fed with a single external feed network.**

I. INTRODUCTION

Simple microstrip antennas radiate linearly polarised fields over a 1-2% bandwidth. By modifying the geometry of the antenna or using a dual feed network with phase shift it is possible to radiate circularly polarised radiation [1,2]. Unfortunately, these changes are permanent and they cannot be used to reconfigure the antennas performance. Electronic control using varactor diodes as oscillators [3] or variable transmission line lengths [4] has been demonstrated. In [5] it was also demonstrated that by changing the number and location of shorting posts both the operating frequency and polarisation of the patch could be controlled. All these techniques require a continuous and precise supply of DC bias and accurate positioning of diodes on the patch surface or addition of phase shifting networks near the patch antenna; all of which perturbs the radiated field shape and polarisation purity. In this paper these disadvantages are overcome by using RF MEMS [6,7] switches integrated into the patch antenna ground plane and connected with shorting vias to the upper plate. Compared with pin or varactor diodes, MEMS consumes little DC power and have low insertion loss and high isolation.

A GPS polarisation reconfigurable patch antenna has been experimentally investigated using RF MEMS switches. The antenna was also located on a stacked high impedance surface (HIS) and its design and analysis was reported in [8]. A square patch antenna design was used, shown in Fig. 1, with four pairs of permanent shorting vias for obtaining four different polarisations. The design is then similar to one given in [5] that used removable shorting posts. Here, the effects of MEMS integrations and parasitic bond wires on antenna performance are quantified and compared with an identical patch antenna using removable shorting posts.

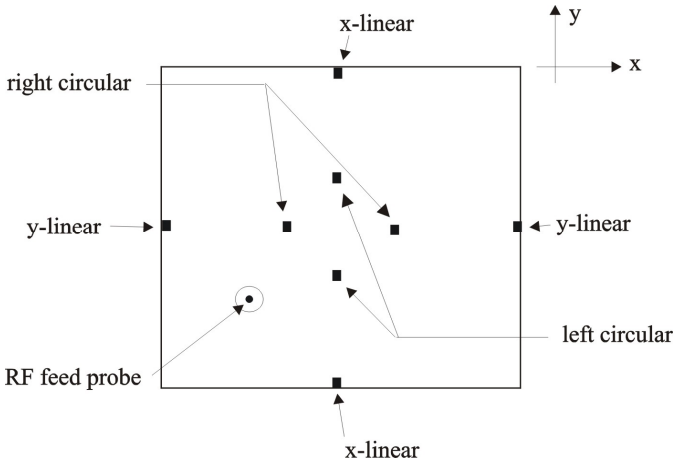

Fig. 1 Square patch antenna with four pairs of posts for obtaining four different polarisations.

The square patch antenna is fed along the diagonal with shorting vias located along the center-line. The shorting vias are connected to the top surface of the patch and plated through the substrate to a small DC isolated pad in the ground plane. The antenna will radiate *x* or *y* orientated linear polarisation, RHCP, or LHCP depending on the location of the vias and whether they are MEM switched "on" (short circuit) or "off" (open circuit). To obtain one polarisation state requires two vias short circuits actuated using either a dedicated MEMS (eight switches) or pairs of ganged MEMS (four switches).

The reconfigurable polarisation control can be explained from a frequency tuning perspective. The square patch without shorting via supports both *x* and *y* oriented modes of the same resonant frequency. Because the feed is located in the diagonal plane it excites both modes with equal amplitude and phase. By switching the appropriate post along the center line $x=a/2$, the resonant frequency of the *y*-orientated mode can be raised without effecting the *x*-orientated mode. A similar arrangement along the *y* orientated mode is used to raise the *x* directed mode. Essentially, the resonant mode with the desired linear polarisation is selected by shifting the

frequency of the orthogonal (undesired) mode further away. The largest frequency shift is obtained by placing shorting posts at, or near, the edges of the patch.

Circular polarisation is obtained by causing the antenna to resonate at two frequencies, both the *x* and *y* orientated modes are excited with equal amplitudes but with 90° phase difference. This is accomplished by raising the resonant frequency of one mode slightly above the other and operating at a frequency between the two resonances. The input impedance of one mode is slightly inductive and the other slightly capacitive. By adjusting the difference in resonance frequency both modes can be excited with equal amplitude. This design is simple and economical but while the impedance matching bandwidth can be increased using either an aperture coupled or proximity fed method, the axial ratio bandwidth remains fixed, typically around 1%.

The use of two feed points generally gives much better axial ratio control than a singly fed patch element, since the amplitude and phase of the relatively polarised field components is determined by the bandwidth of the power divider circuit. However, insertion of a power dividing network would require either an additional circuit board located beneath the antenna or printed adjacent the antenna. Insertion of a power divider will increase losses and if located on the surface perturb the radiate field.

II. MEMS Patch Antenna Design

A. Design and Simulation

The square patch antenna was modelled using a modal expansion cavity resonator model [9]. The results from the model can be used to locate the position of the impedance port which lies along the inter-cardinal or diagonal axis. Consider a patch of arbitrary cross-section of width *a* and length *b* with dielectric thickness *t* and relative dielectric constant ε_r. The electric field under the patch can be computed for the TM_{mn} mode using,

$$E_z(x,y) = jI_o Z_o k \sum_{m=0}^{\infty}\sum_{n=0}^{\infty} \frac{\psi_{mn}(x,y)\psi_{mn}(x_o,y_o)}{k^2 - k_{mn}^2} \qquad (1)$$

where $Z_o = \sqrt{\mu/\varepsilon}$, $k = \omega\sqrt{\mu\varepsilon}$, $k_{mn}^2 = k_m^2 + k_n^2$ and ψ_{mn} are the mode amplitude coefficients and ortho-normalised electric field mode vectors, and I_o the impressed current. For a cavity with perfect magnetic walls,

$$\psi_{mn} = \frac{\chi_{mn}}{\sqrt{ab}}\cos(k_n x)\cos(k_m y) \simeq \frac{\chi_{mn}}{\sqrt{ab}}\cos(\frac{n\pi x}{a})\cos(\frac{n\pi y}{a}) \qquad (2)$$

$$Z_{in}(x,y) = jZ_o kt \sum_{m=0}^{\infty}\sum_{n=0}^{\infty} \frac{\psi_{mn}^2(x_o,y_o)}{k^2 - k_{mn}^2} \cdot G_{mn} \qquad (3)$$

where

$$G_{mn} = \frac{\sin(n\pi d_x)/(2a)}{(n\pi d_x)/(2a)} \cdot \frac{\sin(m\pi d_y)/(2b)}{(m\pi d_y)/(2b)}$$

where, G_{mn} represents the effect of the feed and the product $d_x d_y$ represents the cross-sectional area of the feed.

Using a Taconic circuit board of thickness *t*=1.52 mm and relative dielectric constant ε_r=3.5, tanδ = 0.0018, the *x*-directed TM_{10} mode resonance at f=1575.42 MHz occurs for a patch of physical length 5.0547 cm, with a computed quality factor of Q=84. The series was truncated for the first *m*=*n*=3 modes. The ratio of orthogonal frequencies was in the range 1.01-1.10 depending on the VSWR bandwidth definition. The bandwidth is primarily a function of the thickness and dielectric constant of the substrate. The computed -10 dB bandwidth was 14.8 MHz or 1%. The *y*-directed TM_{01} mode occurs for W=4.947 cm. Fig. 2(a) shows the computed impedance plot for the TM_{01} and Fig. 2(b) shows the impedance contours for the orthogonal TM_{10} mode. The contours though very similar do have subtle differences. Overlaying the two impedance contour maps and locating the co-ordinates where the 50 Ω contours intersect determines the location for an impedance port. This was found at 15.9 mm from the resonant *y*-edge and 16.8 mm from the resonant *x*-edge of the patch.

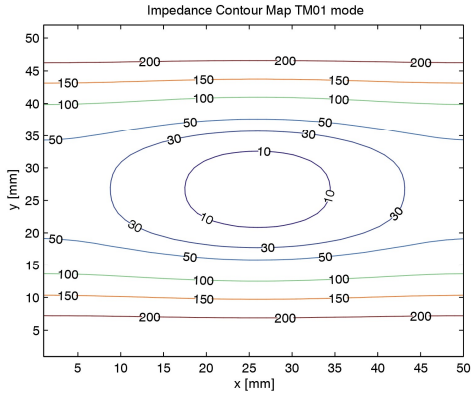

(a)

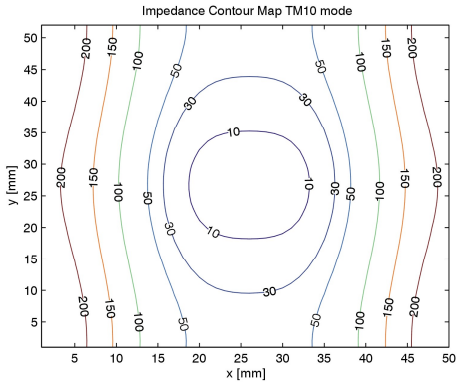

(b)

Fig. 2 Impedance contours of the GPS patch antenna (a) TM_{01} mode (b) TM_{10} mode.

To verify the dimensions and the modal switching action of the short circuits it was decided to implement an HFSS model. The full wave model readily facilitated computing the radiated fields and more accurately the cross-polarisation and axial ratio levels. Moreover it allowed field diagnosis and enabled a better understanding of the impedance matching. The patch antenna was modelled on a finite ground plane of 8x8 cm square surrounded by a cuboid of super absorbing boundaries. Table 1 summaries the computed antenna matching bandwidth and cross-polar field levels. When one considers practical patch antenna radiated fields the predicted cross-polar isolations and axial ratios should be considered ideal. The return loss on the feed matching remained unaltered and in one configuration even enhanced. In the case of horizontal and vertical switched modes the presence of another mode was observed around 1.3-1.4 MHz that was weakly excited.

Polarisation	Freq. [GHz]	S_{11} [dB]	X-pol [dB]
Horizontal	1.59	-12.6	-24.5
Vertical	1.57	-11.1	-25.1
RHCP	1.59	-12.5	-0.3
LHCP	1.60	-28.5	-0.1

Table 1. Summary of computed resonant frequency, peak insertion loss and cross polarisation levels for the reconfigurable patch antenna.

Table 1 indicates that the resonant frequency tends to shift above the 1575 MHz operating frequency. In practice this shift can be post fabrication retuned to the desired frequency using small tuning stubs. A prototype patch antenna was fabricated and its impedance and radiated field patterns measured for the various polarisations by close circuiting the appropriate plated vias. Table 2 summarised the measured performance of the reconfigurable patch antenna in the various polarisation states. The patch antenna resonance frequency was observed to shift slightly for different wire configurations switched “on” and “off”. The differences in resonance frequency are due to the fact that the wire has less inductance than that of the 1 mm square metal posts used in the simulation. The linear polarisation state bandwidth was typically 1% and the CP approximately double 2%.

Polarisation	Freq. [GHz]	-10[dB] BW (MHz)	X-pol [dB]
Horizontal	1.575	14.1	-16.5
Vertical	1.550	12.0	-17.5
RHCP	1.570	34.9	-0.5
LHCP	1.566	30.0	-0.7

Table 2. Summary of measured resonant frequency and impedance matched bandwidth for the reconfigurable patch antenna.

MEMS Patch Antenna

Fig. 3 shows the four Dowkey M1C06-CDK2 RF MEMS switches [10] attached to the plated vias on the patch antenna ground plane. To produce each polarisation state required two via short circuits to be opened or closed using one MEMS switch. Ganging the MEMS in this way created some parasitic effects but reduced the cost and integration complexity.

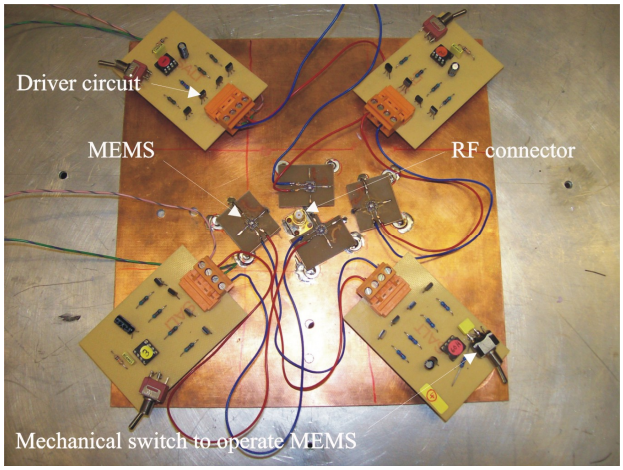

Fig. 3 Picture of the patch antenna ground plane showing four MEMS and driver circuits integrated.

A. Input Impedance

Fig. 4(a) shows the insertion loss for the linear horizontal polarisation state. The mode is raised at the desired GPS frequency and bandwidth. The mode has not shifted appreciably in frequency, as any electrical length added by MEMS tracks and bond wires to the shorting vias is nearly identical. However the impedance match has decreased by about 10 dB and the bandwidth has been narrowed. The origin of this mismatch was traced to the impedance transitions on the MEMS circuit pads.

Fig. 4(b) shows the insertion loss for the right hand circular polarisation state. The quality of impedance match is seen to be again reduced by a similar order of magnitude as in the linear polarisation case. The centre of the double resonance frequencies is located at 1.579 GHz. Interesting, with two modes arranged to be so close it proved relatively easy to obtain circular polarisation.

B. Radiation Pattern

Fig. 5(a) and (b) show some typical measured radiation patterns for the MEMS patch antenna switched between linear and circular polarisation modes. The field patterns show decreased polarisation isolated and axial ratio compared to the patch antenna using ideal shorted vias. The linear polarised field is symmetric with an isolation of better than -12 dB for both horizontal and vertical planes, and the left hand circular polarised field axial ratio is less than 1.2 dB over a wide angular sector around the zenith.

CONCLUSION

Integration of MEMS switches with printed antenna technology allows reconfigurable electronic control of patch antenna polarisation to be obtained. Parasitic effects of bond wires and any impedance transitions from the MEMS switch to the antenna should be minimized as far as is possible. Using RF MEMS continuous bias control and drift problems

associated with varactor diode integration is avoided and the antenna is capable of operating in high power transmit applications. Modification of printed antenna technology in this way may sacrifice some ease of construction. However the additional capabilities afforded by these modifications should offset the increased complexity and cost of fabrication.

ACKNOWLEDGMENT

The authors would like to acknowledge the financial support of Dstl under grant No. RD/0297996.

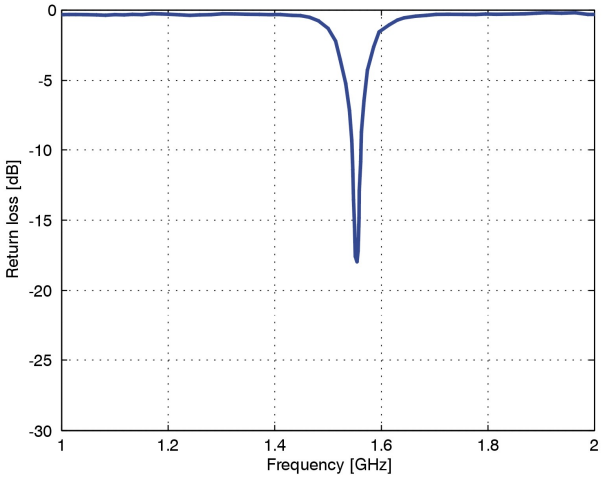

(a)

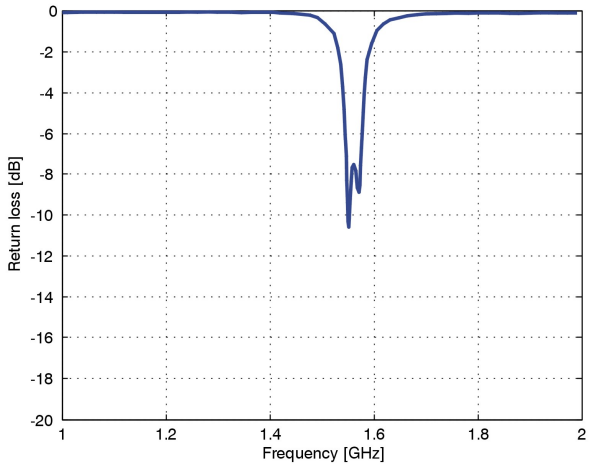

(b)

Fig. 4 Measured insertion loss for the patch antenna using integrated MEMS in two polarisation states. (a) linear horizontal polarised (b) left hand circular polarisation.

REFERENCES

[1] J. Hang, "Techniques for an array to generate circular polarized Radiation with linearly polarized elements", IEEE Trans. On Ants. And Propagat., Vol. 34, pp. 113-1123, 1986.

[2] P. S. Hall, "Review of techniques for dual and circular polarized microstrip antennas", *Microstrip Antennas: The Analysis and Design of Microstrip Antennas and Arrays*, New York, IEEE Press, pp. 107-117, ISBN 0-7803-1078-0.

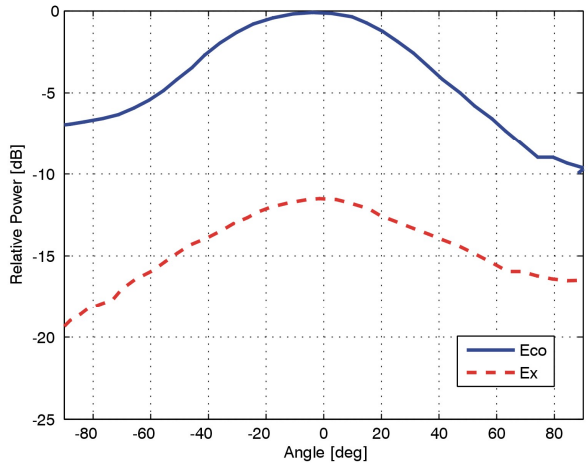

(a)

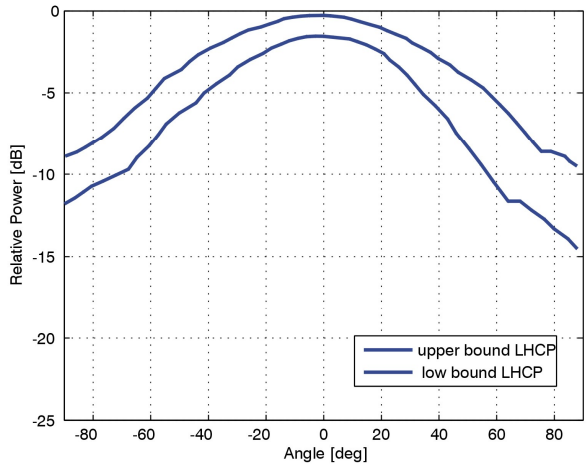

(b)

Fig. 5 Measured radiation pattern for linear horizontal polarised patch antenna using integrated MEMS at 1.57 GHz. (a) E-plane (b) H-plane.

[3] P. Haskin, J. S. Dahele and P. S. Hall, "Polarisation agile active patch antenna", IEE Electronics Lett., vol. 30 pp.98-99, 1998.

[4] J. L. Kerr, "Terminated microstrip antenna", in Proc. 1978, Antennas Application Sym. Univ. of Illinois, Sept. 1978.

[5] D. H. Schaubert, F. G. Farrar A. Sindoris and S. T. Hayes, "Microstrip antennas with frequency agilty and polarisation diversity", IEEE Trans Ants and Propagat. Vol 29, No. 1, pp. 118-123, Jan 1981.

[6] B. Cetiner, H. Hafarkhani, J. Qian and H. Yoo, "Multifunctional reconfigurable MEMS integrated antennas for adaptive MIMO systems", IEEE Comms Mag. Pp. 67-70, Dec. 2004.

[7] G. Huff and J. Berhard, "Integration of packaged RF MEMS switches with radiation pattern reconfigurable microstrip antenna", IEEE Trans. On Ants and Propagat. , vol. 54, No. 2 pp. 464-469, 2006.

[8] N. Clow and I. L. Morrow, "Effect of high impedance substrate on circular polarised patch antennas radiated fields", IET Wideband Symposium, 2008.

[9] K. R. Carver and J. W. Mink, "Microstrip antenna technology", IEEE Trans. On Ants. And Propagat. , vol. 29, pp. 2-24, 1981.

[10] Dow-Key Microwave Corp., 4822 McGrath St., Ventura, CA 93003-7718,Internet, www.dowkey.com